UNIVERSITY OF HOUSTON

3-D Paleochannel Reconstruction and Paleocurrent Fields of Cretaceous Ferron Meanderbelts, Henry Mountains Region, Utah (U.S.A.)

By Jianqiao Wang, Advisor: Janok Bhattacharya

4/6/2012

Abstract

Plan view and cliff exposures of an ancient meander belt in the Cretaceous Ferron Sandstone member, Mancos Shale Formation, Utah, allow us to test numeral models of facies variability in meander belts. These models predict that grain size and vertical facies associations vary as a function of the style of bar migration (translation vs. expansion) as well as position within a bar (upstream vs. downstream). This project will integrate measured sections and bedding diagrams of cliff exposures with areal mapping of grain size and paleocurrent variability to investigate the plan view variations in grain size as a function of paleoflow. The study will also evaluate empirical estimates of meander wavelength and channel sinuosity, and other hydraulic parameters (average velocity, mean discharge, bankfull channel depth) by interpreting more traditional outcrop data (thickness and cross-sectional dimensions of bedforms and bars) with the data measured in the plan-view exposures (meander wavelength and channel sinuosity).

Introduction

Many studies of ancient and modern rivers involve paleochannel reconstruction from 2-D or 3-D point bar models (Pranter, et al., 2007; Shukla, 1999; Willis, 1989; Willis and Tang, 2010). Point bar computer modeling predicts 3-D geometry, grain size variation, and connectivity of point bar deposits (Fig.1 and Fig. 2), and they are controlled by the interaction of sediment supply and flow. However, nearly all input parameters (channel discharge, sediment density, mean sediment grain size, and et al.) are held constant during the simulation of synthetic point bar deposits. Such numerical models have limitations that may not be applicable in every natural river. For instance, Willis's 2-D model (1989) was only compared with observations of point bars in symmetrical, fine to medium grained channel bends. Many modeling results indicate that the interpretation needs more detailed facies and geometry descriptions of field examples.

Willis (1989) also showed that paleocurrent variations within point bars can be produced by the interaction of channel geometry, channel migration pattern, and relative outcrop orientation. Results predicted through numerical modeling can be tested against field examples. In all the 2-D cases simulated by Willis (1989), point bar sequences become thicker away from the meander belt axis, toward the bend apex (Fig. 2). Variability in thickness of point-bars depends on the bend sinuosity (Willis, 1989). Point bars accrete laterally and downstream. As point bars become thicker laterally, the surface of laterally accreting bedsets tend to steepen and be more concave upwards (Fig. 2). As a point bar migrates downstream, grain sizes coarsen upward in the upstream part of the bends and fine upward in the downstream part of the bends (Willis, 1989). Modern fluvial deposits (Fig. 3 and Fig. 4) also show great variance in paleocurrent direction (Shukla, et al., 1999)

Point bar deposits need to be described in terms of lateral variation in bedset thickness, 3-D geometry, grain size, sedimentary structures, and paleocurrent directions (Willis, 1989). Point bars are so complex that it is difficult to differentiate spatial and temporal variations using traditional 2-D vertical outcrops (Willis, 1989). Great caution should also be paid to reconstruct ancient channels using well log data or core data. Willis (1989) suggested that paleocurrent indicators in the upper ~10-20% of fining upwards point-bar sequences are not as reliable as the ones located in the lower parts of individual bedsets.

Methodologies like seismic time-slice and well data analysis have limitations. Seismic time-slice analysis is ambiguous in the vertical dimension, due to the seismic resolution problem (Reijenstein, et al., 2011), and limited subsurface-well data interpretation is uncertain in identifying the connectivity of sand bodies in channel belts (Bridge and Tye, 2000; Miall, 2006,)

Due to these issues in modeling and limitations of traditional 2-D studies and seismic time-slice, geometrical complexities in outcrops need to be documented for the accuracy of paleochannel model reconstructions (Willis, 1989). Lots of field work has been done to document fluvial deposits in the Ferron sandstone, and 3-D architecture descriptions in fluvial deposits have been completed in a few studies (Barton, et al., 2004; Bhattacharya and Tye, 2004; Bhattacharya and MacEachern, 2009; Corbeanu, et al, 2004; Garrison and Van den Bergh, 2004; Van den Bergh and Garrison, 2004). However, little work has been done on reconstructing ancient channels in association with outcrops with plan-view exposures. Few articles discuss relationships between large exposed meandering scrolls and associated vertical exposures.

Cretaceous fluvial deposits near the north end of Nielson Wash (Hansville, Utah) expose both cliff and plan view geometry of ancient lateral accretion deposits and channels. Paleohydraulic estimates suggest that Ferron rivers are not continental rivers and that they are partly fluvial dominated and partly tidal dominated, and the trunk river depths are about 6 to 9 meters (Bartor, et al., 2004; Bhattacharya and Tye, 2004; Bhattacharya and MacEachern, 2009; Garrison and Van den Bergh, 2004; Li, 2010). It is thus timely, to review the Ferron as an analog for fluvial-deltaic reservoir modeling considering these recent findings, and address the following problems. What is the range of scale of Ferron rivers? What is the 3-D geometry of point bars? How does the extent of mud drapes vary? In order to determine the spatial and age relationships of the exposed point bars, and characterize the reservoir heterogeneity, all these problems need to be solved, especially using the spatial variability of paleocurrent direction in plan-view.

In our study area, it is difficult to observe vertical and lateral variations in each bedset other than the very top of the exposed meander belts. The plan-view data collected from exposed lower and middle point bar may be more reliable than those traditional ones, such as cross beddings, flute casts, parting lineations.. Therefore, it is valuable to observe paleocurrent data in plan view (initial results show in Fig. 5 and

Fig. 6), and illustrate how the vertical and the horizontal views of an outcrop relate to each other.

The limitation of 2-D outcrops can be removed by using high resolution geophysical techniques. GPR may play a key role in interpreting 3-D deposit variations in our study area. Ground-penetrating radar is a powerful geophysical technique with high resolution that can detect shallow subsurface stratigraphic features, such as bar accretion surfaces. Several articles make use of GPR to evaluate the medium-to-large scale structure of point bar deposits in 3-D (Bridge, et al., 1995; Corbeanu, et al., 2004). Achieving a more complete view of the subsurface with GPR imaging requires good resolution with vertical spacing of decimeters (Bridge, et al., 1995). Ground-penetrating radar may provide an unparalleled view of lateral bar accretion, downstream accretion, and allow construction of the spatial distribution of ancient channel deposits through time (Mukherjee, 2012).

Miall (1994, 2006) demonstrated that the best method for defining the scale of a river is the size of its architectural elements as measured in outcrop (Fig. 7 and Fig. 8). The other major practical methods, such as tectonic setting, climate and the study of sedimentary provenance, may not be as reliable predictors of fluvial scale, compared to direct outcrop observation (Davidson and Hartley, 2010; Miall, 2006).

Continental-scale fluvial systems (such as the Ganga and Mississippi rivers) are characterized by large-scale depositional elements, such as large-scale crossbed units, channel widths up to 20 km, depths up to 40 m, deep scours, which may be up to 5 times average channel depth, especially at channel confluences, and mesoforms (large dunes) up to at least 5 m high (Miall, 2006). These criteria can be used for estimation of the size of smaller Ferron rivers. Certain equations may be used to calculate the original depth and width of an ancient river with field data. There also exists a challenge when predicting channel depth in vertical exposed outcrops because the upper finer parts of channel fill deposits are hard to preserve during channel avulsion. So the upper bars may not be preserved in the outcrops. These have important implications for current methods of paleochannel reconstructions and studies of reservoir heterogeneities. This intergration of point bars models conditional to field data may be need to represent channel-fill architecture very well, and it may be helpful in simulating 3-D reservoir models (Foster, et al., 2004)such as the 2-D and 3-D petrophysical models with data collected from Willims Fork Formation, Piceance Basin, Colorado (Pranter, et al., 2007).

Ferron sandstone outcrops have been used as analogs to petroleum reservoirs in the Gulf of Mexico (Knox, 1997), Alaska (Bhattacharya and Tye, 2004) and elsewhere. The high complexity of Ferron rivers allows documentation of heterogeneity within sandstone point bars. This is a key issue in dealing with petroleum reservoirs.

The extent of mud drapes differs greatly in fluvial dominated and tidal dominated deposits. Tidal cycles are monthly and daily, and consequently, there is more chance to get more numerous and more extentsive of mud drapes (Bridge, 2003; Corbeanu, et al., 2004). By looking at inclined heterolithic strata (IHS) on laterally accreting point bars in 3-D, it is possible to test the hypothesis of mud drape extent as a function of the estimated paleohydraulic parameters. IHS comprises cross laminated sandstones separated by mudstones. The mudstone interbeds may be generally continuous, and drape the entire bar from top to toe (Corbeanu, et al., 2004), they may also overlay the top of the sand body, the latter type of drapes are called flood drapes. Flood drape deposits bound each flooding story, and represent the 4^{th} to 5^{th} order bounding surface of migrating point bars (Miall, 1988). The 1^{st} and 2^{nd} order ones respectively bound individual crossbed sets and cosets of similar cross bed facies, and the 3^{rd} order bounding surface represents the reactivation of macroforms (Miall, 1988).

Variation between fluvial dominated and tidal dominated channel deposits may be indicated by the extent of a mud drape. Tidal mud drapes are recorded in migrating tidally-influenced channels. The laterally accreting point bar has thick mud layers from slack flow during tides (Galloway and Hobday, 1996; Mackay and Dalrymple, 2011). The typical mixed bedding under tidal control indicates flow strengths of the tide. Flaser bedding in sandy inclined strata is a result of low suspended sediment deposition. Mud is only preserved in the trough of the bedform. As mud content increases, wavy bedding may occur, composed of continuous sand and mud layers. Lenticular bedding is mainly mud with bits of sand (starved isolated ripples), owing to high suspended sediment deposition (Mackay and Dalrymple, 2011). The importance of these signatures is clear. For example, when analyzing the ancient record, based on the overall geometry and facies characteristics, it is possible to interpret point bars as tidal influenced meander scrolls. Reactivation surfaces in sand/mud couplets near bar tops may indicate tidal reworking. In summary, mudstones in non-overbank deposits may show evidence of intermittent flow (Smith, et al., 2009). Finer-gained deposits occuring in sigmoid sandy strata may be an indicator of tidal influence. Otherwise, inclined units of siltstone on the top parts of channel deposits may be interpreted to be counter point bars, which are supposed to be fluvial-dominated (Jones and Hajek, 2007; Smith, et al., 2009). Counter point bars typically consist of silt-sized sediment, and form on the distal downstream end of a normal point bar, before the cut bank (Smith, et al., 2009). They are easy to recognize in modern fluvial deposits, although there is sparse literature documenting ancient counter point bars. Such counter point bars are different from common point bars in terms of the concave accretion surfaces in a downdip direction, shown in the plan view (Smith, et al., 2009), and contrasting with the convex curvature of point bar surfaces (Miall, 1994).

These signatures of counter point bars or IHS tidal drapes are expected to be found in our vertical cliff exposures. These may provide the foundation for heterogenous mud layers in estimating the dimensions and morphology of petroleum reservoirs, such as in the Mcmurray Formation of Alberta Tar Sands (Labrecque, et al., 2011; Tye, 2004

Geological Setting

The Late Cretaceous Notom Delta belongs to the Ferron Member Sandstone of the Mancos Shale Formation, which is mostly deposited in a high stand system tract

(Li., et al., 2011). The meander scrolls exposed in the study area belong to sequence 1 in the regional sequence stratigraphic study (Li, 2011; Zhu, 2010; Zhu, et al., in press), in which 43 paasequences, 18 parasequence sets, and 6 sequences are identified (Fig. 9 and Fig. 10). The Notom delta is one of several delta complexes formed after 91.25 Ma, which consist of the Notom delta, the Last Chance delta, and the Vernal delta, all of which were derived from the Sevier Orogenic belt and deposited in the Western Interior Seaway towards the northeast (Fig. 11), in a humid to subtropical setting (Bhattacharya, 2004; Gardner, 1995; Li, et al., 2010; Li, et al., 2011; Zhu, et al, in press).

Study Area

The outcrop is located near the north end of Nielson Wash (Hanksville, Utah), see Fig. 12. The exposures are composed of several cliffs ranging from 5 meters to 2 meters in height and several meander scrolls can be seen in plan-view. One major cliff exposures is about 150 meters long, which gives a cross-sectional view of a channel belt and enables description of vertical sedimentary facies of the ancient fluvial system. The other major cliff exposures are along the edge of the point bar margins. They are partly weathered but show great variance in grain sizes, which can be used to compare the age relationship between point bars.

Largely exposed sandstone meander scrolls in plan-view provide the opportunity to reconstruct the paleohydraulics of the Cretaceous point bars. Paleocurrent measurements on top of the channel belt should show the flow direction and spatial variability.

Methods and Data

The simulations and equations presented by Willis (1989, 1993a), and Willis and Tang (2010) can be compared to ancient point bar deposits. Grain sizes and elevations of bar deposits are all marked in tens to hundreds of meters increments across the modeled point bar deposits. Some can be clearly seen by examining the geometry in outcrop, as well as through geophysical techniques like ground-penetrating radar (GPR). Within an outcrop it is common to observe systematic vertical and lateral variations (Willis, 1989).

Specific data, like thickness of individual bar deposits, will be documented by measuring the sections along cliffs and it may result in the reconstruction of channel flow depth and flow velocity based on bedding diagrams and the 3-D bedform phase diagrams (Bhattacharya and Tye, 2004). Facies description along the 150 meters long vertical cliff provides supporting information for 3-D reconstruction of ancient river deposits, including grain sizes and sedimentary structures within laterally accreting bedsets. The geometry of successive lateral accretion surfaces within a bar deposit can be obtained in plan-view and cross sectional exposures. Point bar migration patterns can be obtained from a detailed examination of meander scrolls (accretion topography, grain size and paleocurrent direction measurements). The more the channel migrates, the more the amalgamated sand bodies are side-attached. Moreover, bedding architecture and paleocurrents can be used to distinguish longitudinal and / or transverse bars in braided rivers versus migrating point bars in meandering rivers (Fig. 8). These bar types can be distinguished in outcrops. Meandering rivers migrate in the form of expansion, translation, or a combination of both.

Such detailed 3-D description and interpretation of these large scale features of point bar deposits is also possible through the use of GPR profiles. Additionally, our plan-view and cross sectional outcrop provide more dimensional data to estimate the original bankfull depth of the Ferron rivers, comparied to the 2-D outcrop documented in Bhattacharya and Tye (2004) and Li, et al. (2010).

Original bankful channel depth, original bankful meandering width, and meander-belt width can be estimated through dimensions of a single fluvial sand body in outcrop (Fig. 13) by applying these equations: $D=D^{*}\times0.585/0.9$, (Ethridge and Schumm, 1977), where D = Original bankful channel depth, D* = Average thickness of the main point bar; $W=W^{*}\times1.5$, (Allen, 1965), where W = Original bankful meandering width, W* = Average horizontal width of the lateral-accretion surfaces as exposed in outcrop.

Moreover, it should be possible to measure the meander wavelength and contrast this with estimates made using parameters taken from cliff exposures (Fig. 5 and Fig. 6) using equations here: $\lambda m=10.9W^{1.01}$(units=m), (Leopold and Wolman, 1960); $\lambda m=18(F^{0.53}W^{0.69})$ (F=W/D; units=m), (Schumm, 1972), where λm = Meander

Amplitude (meander-belt width), W = Bankfull channel width, D = Original bankful channel depth, F = Bankfull channel width-to-depth ratio.

These empirical equations are based on analogs of modern systems, and have been used to relate outcrops dimensions that are potentially preserved in the geologic record to estimate paleohydraulic parameters. We can actually observe features like meander amplitude and channel width in our plan-view exposures, so we can test the equations with our ancient examples.

Here are the methods of estimating river discharge. $Q = A \times U$, where Q = Discharge, A = Cross sectional area of the channel (Width × Depth), U = Average velocity, later articles applied the equation demonstrated by Matthai (1990): $\log Q_{flood} = -0.070(\log A^2) + 0.865\log A + 2.084$. (Bhattacharya and Tye, 2004; Bhattacharya and MacEachern, 2009; Davison and Hartley, 2010)

Initial Results

Channel fill facies.—The shape and large-scale structure of the sandstone bodies are illustrated in Fig. 14 and Fig. 15. Some thicker sandstone bodies contain channel-form inclined strata, which pass laterally at their upper edges into thinner wedges of sandstone, which are triangular in shape. The thicker sandstone bodies comprise several large-scale lateral accretion sets (Fig. 14). Medium to large scale planar cross strata, with set thickness ranging from 0.2m to 1.5m, but commonly 0.1 to 0.5m, is the dominant internal structure of the large-scale inclined strata, which is lower medium to lower coarse sandstone. Medium-scale strata, and their upper parts, that are very fine to upper fine sandstone, generally contain planar cross strata or trough cross strata (set thickness is about 0.3m). Within the laterally accreting bars, cross bedding dips in the direction of the paleoflow. The thinner sheet-like sandstone strata (about 1.5m thick) are overlain by mudstone, abundant in iron and which containe *Beaconites* burrows (Fig.18), indicating a quiet paleoenvironment where the channel was abandoned and filled in with shallow fresh water. Medium scale trough cross strata in the upper part (set thickness <0.3m) is the sedimentary structure within the channel margin fills.

Channel margin facies.—Channel margin facies comprise crevasse splays with very fine to fine sandstone deposits. Ripples are observed within sandstone units, thinning away from ancient channel towards the floodplain, with coarser sand deposited on the top.

Interchannel floodplain facies. —The outcrop shows meters thick units of non-bioturbated (BI 0) silty mudstones and interbedded siltstones, preserved in the basal channel margin units. These mudstones are characterized by abundant, centimeter-thick, thin bedded, inverse and normally graded siltstone to claystone couplets (Fig. 16). Allochthonous plant materials, such as amber and pieces of wood, are ubiquitous. These mudstones locally display soft deformation features, particularly at the boundary separating normally graded above and inverse graded below.

The most reliable indicators of paleocurrent direction found in outcrops are rib and furrow structures on the very top surfaces of the point bars (Fig. 17), and large-scale trough cross-stratification and planar cross bedding in vertical cliff exposures (Fig. 14). Measuring all possible attitudes of dipping beds and orientation of cross-bedding will allow the 3-D reconstruction of these ancient channels and their paleocurrent variability.

Preliminary Conclusions

The Ferron rivers are small to medium scale, with more tidal influenced meanders located close to the upstream end of a tidal estuary. “Text-book” style channel and bar geometries constitute most of the Ferron river sandstone in our study area. The lateral amalgamation of many point bars suggests the dominance of a meandering river style, in which sinuosity is moderate to high. There are several stories of channel deposits located in the study area. Ferron channels were migrating in three forms: translation, expansion, and a combination of the two.

Hypothesis

Paleocurrent directions are variable with the position on a bar and they largely depend on the meander loop position and the channel migration pattern (expansion or translation). Evaluation of paleocurrent directions in point bar deposits is quite useful in reconstructing ancient channels, though many scholars argue that traditional studies using paleocurrent directions solely in cliff sections or cores are fraught with uncertainty (Bridge, et al., 2000; Shukla, et al., 1999; Willis, 1989). Integration of paleocurrent data, and plan-form scroll bar geometry may be used to infer migration pattern of ancient point bars. Additionally, rib and furrow structures are more reliable indicators than the sedimentary structures on cross sections, as well as flute casts and parting lineations on the top of beds. Bar drapes may help evaluate heterogeneity of sandstone point bars.

Future Plans

The ultimate goal of this study is to evaluate the paleocurrent directions as preserved on plan-view exposures of ancient point bars and associated cliff exposures. The orientations of dipping beds and cross bedding units will contribute to reconstruction of the geometry of the Cretaceous Ferron rivers. Future plans may include taking as many measurements as we can. Grain size and paleocurrent direction measurements of nearly 200 samples in each single exposed meander scroll are to be collected in the coming summer, in order to examine the accretion topography within meander scrolls. Ground-penetrating radar may be used to help image deposition in 3-D. A more accurate 3-D architecture of ancient fluvial deposits is expected to be built.

Figures

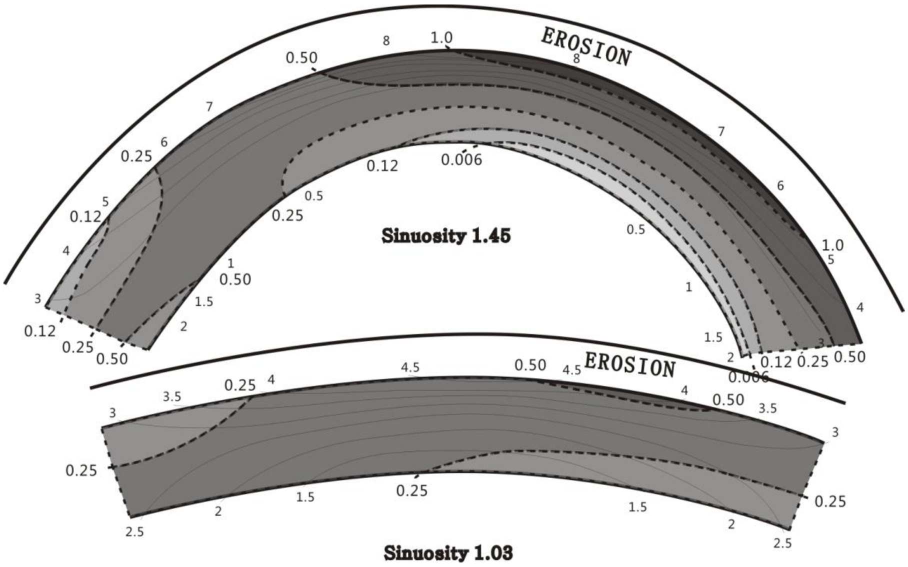

Figure. 1 Two simulated point bars with different sinuosities. The channels have the same discharge, mean centerline depth, width and down valley slope. Solid contours display depth in meters and dashed lines display grainsize in millimeters, revised from (Willis, 1989).

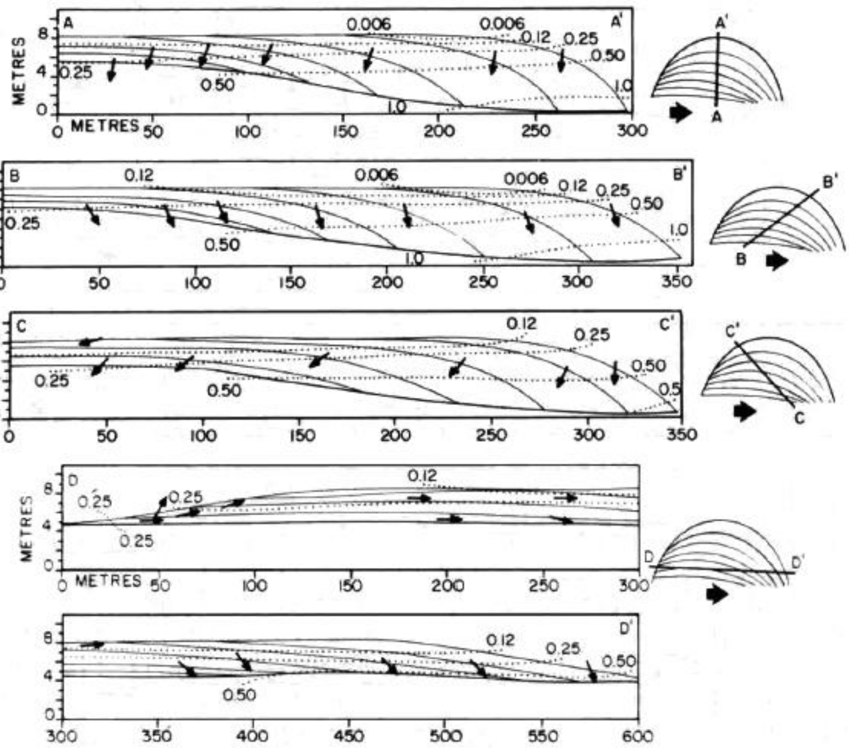

Figure. 2 Cross-sections of simulated point bar deposit formed by down-valley translation and channel-bend expansion (Willis, 1989).

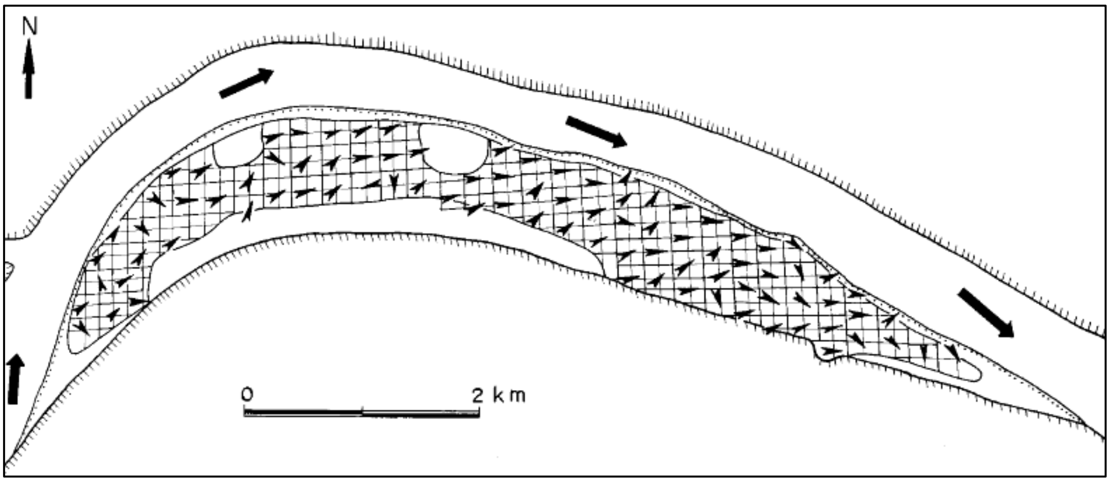

Figure. 3 Moving averages of the paleocurrent trends in sectors on the Saidpur point bar, the Ganga river, India. Each arrow represents the average of four adjacent grids. Flow direction is variable in upstream part (Shukla, et al., 1999).

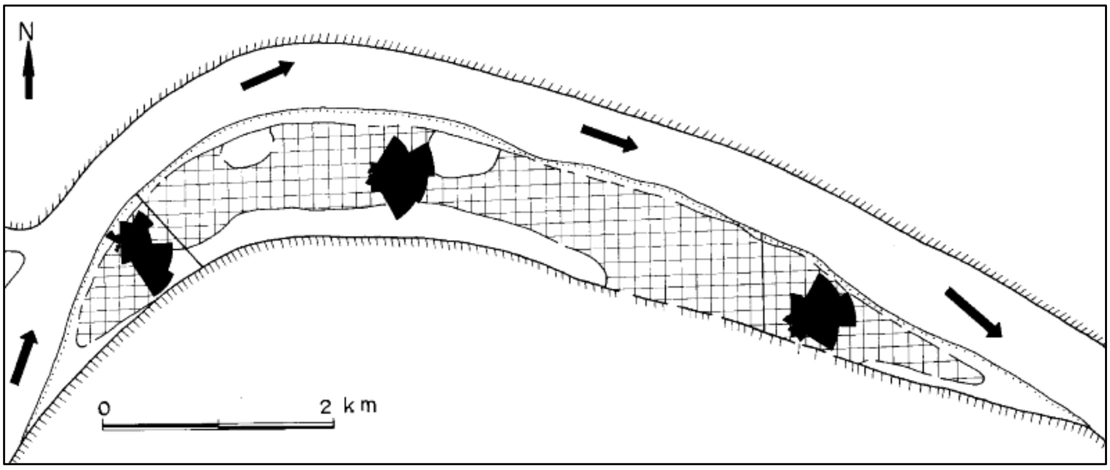

Figure. 4 Paleocurrent trends shown as rose diagram for upstream, middle and downstream segments of the Saidpur point bar, the Ganga river, India (Shukla, et al., 1999).

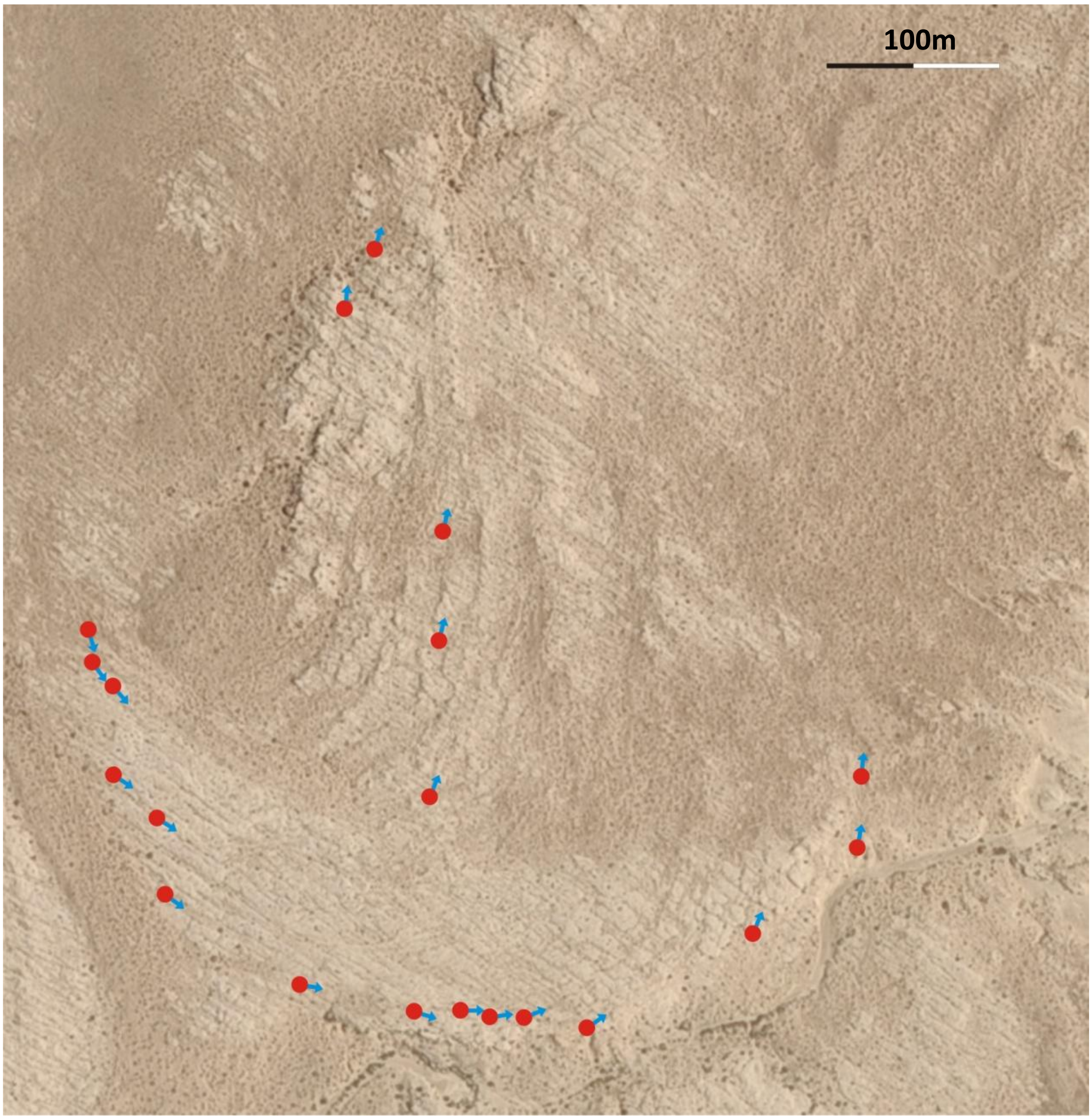

Figure. 5 North bar initial paleocurrent results. Red dots with blue arrow points the measured paleocurrent direction.

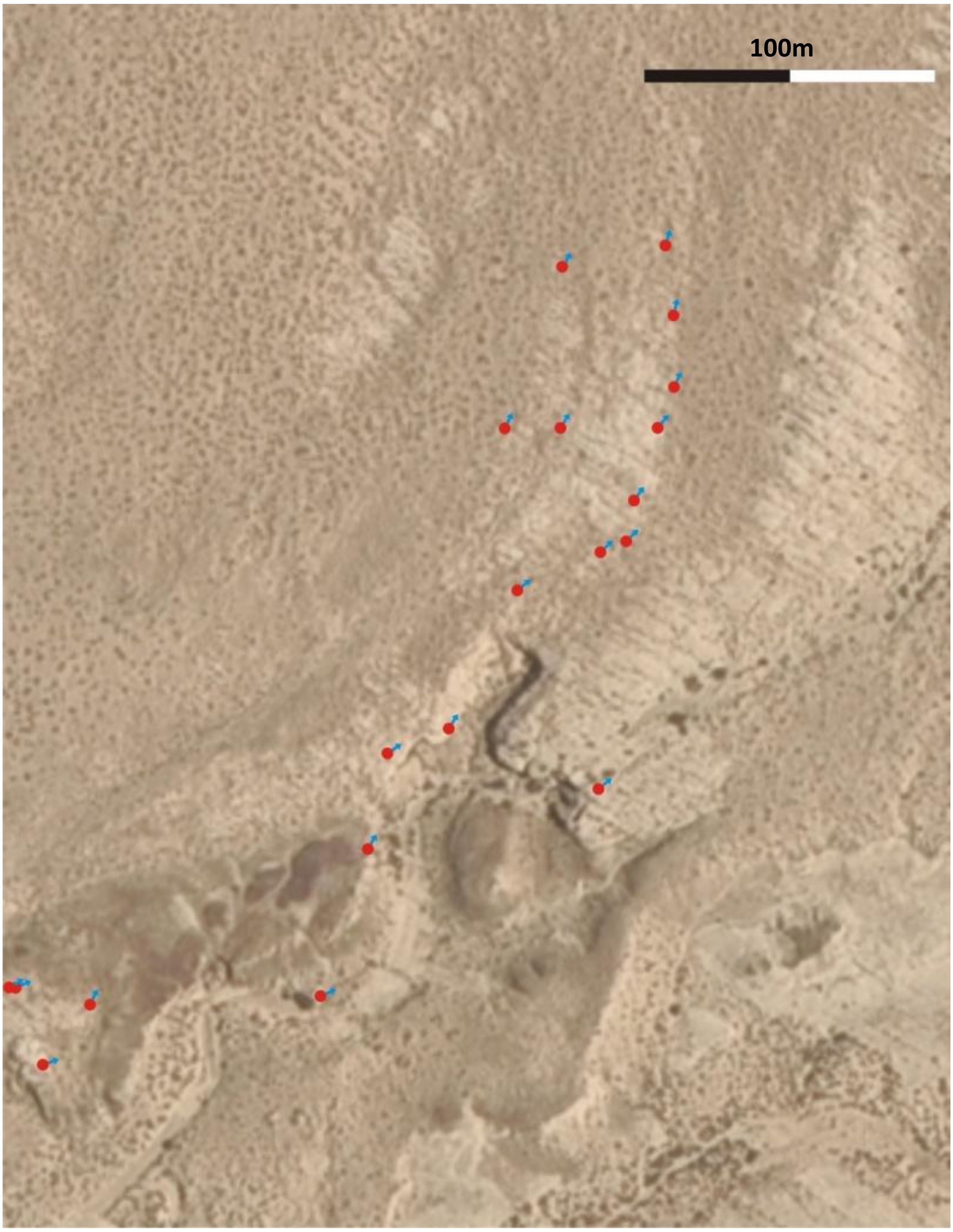

Figure. 6 South bar initial paleocurrent results. Red dots with blue arrow points the measured paleocurrent direction.

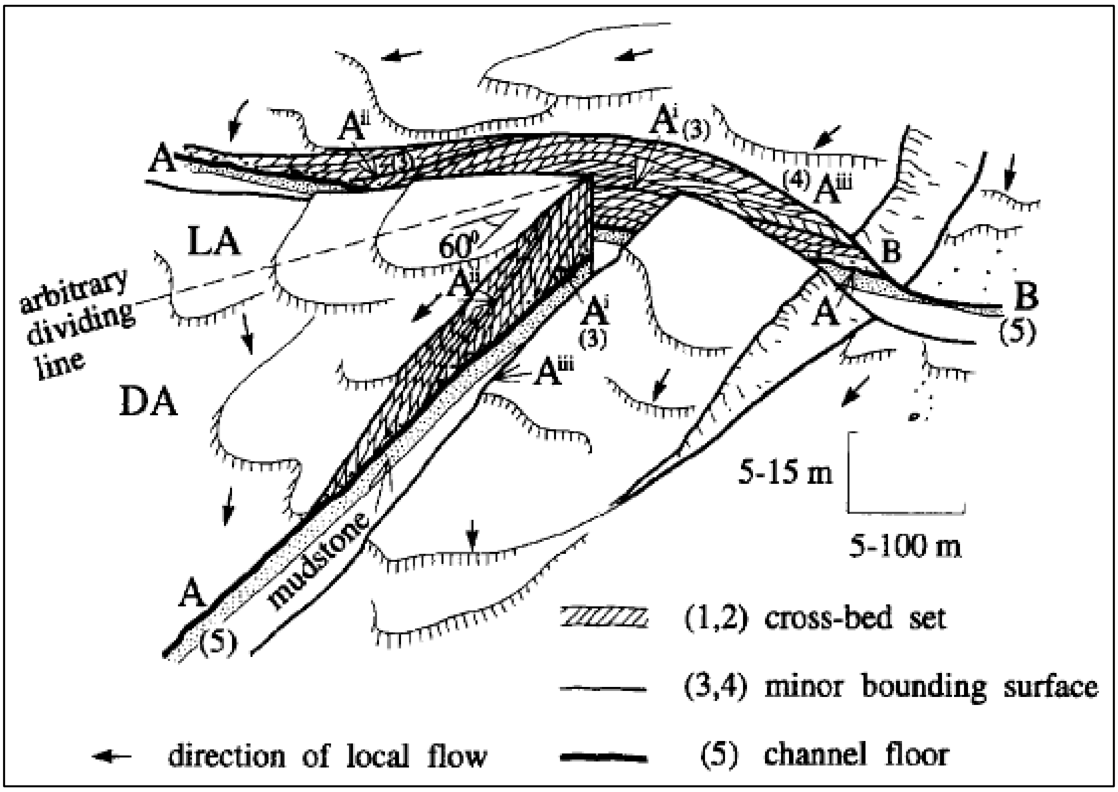

Figure. 7 LA (Lateral accretion), Oblique accretion, DA (Downstream accretion). Figure from Miall, 1994.

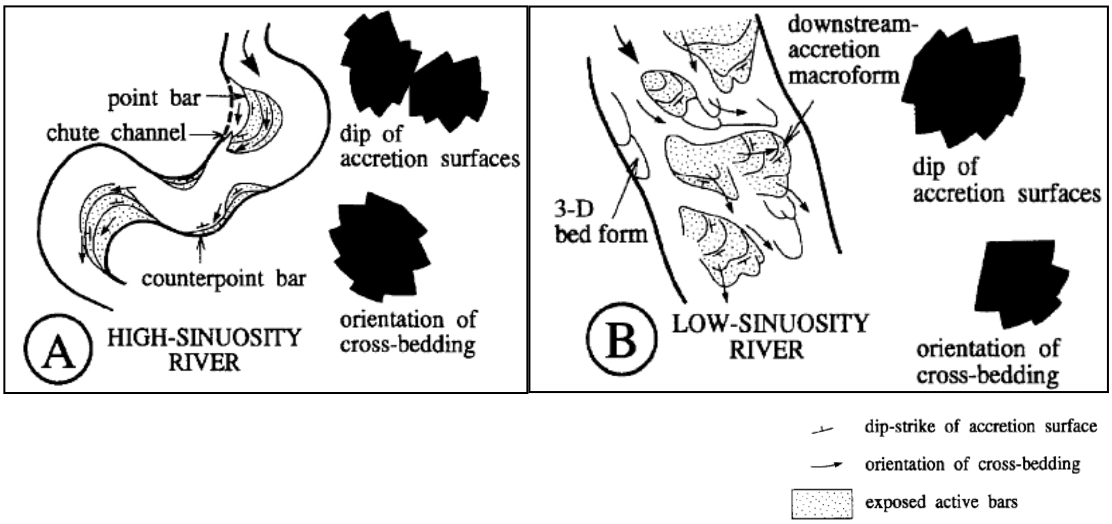

Figure. 8 Models predict fundamentally different paleocurrent patterns versus river type. Figure from Miall, 1994.

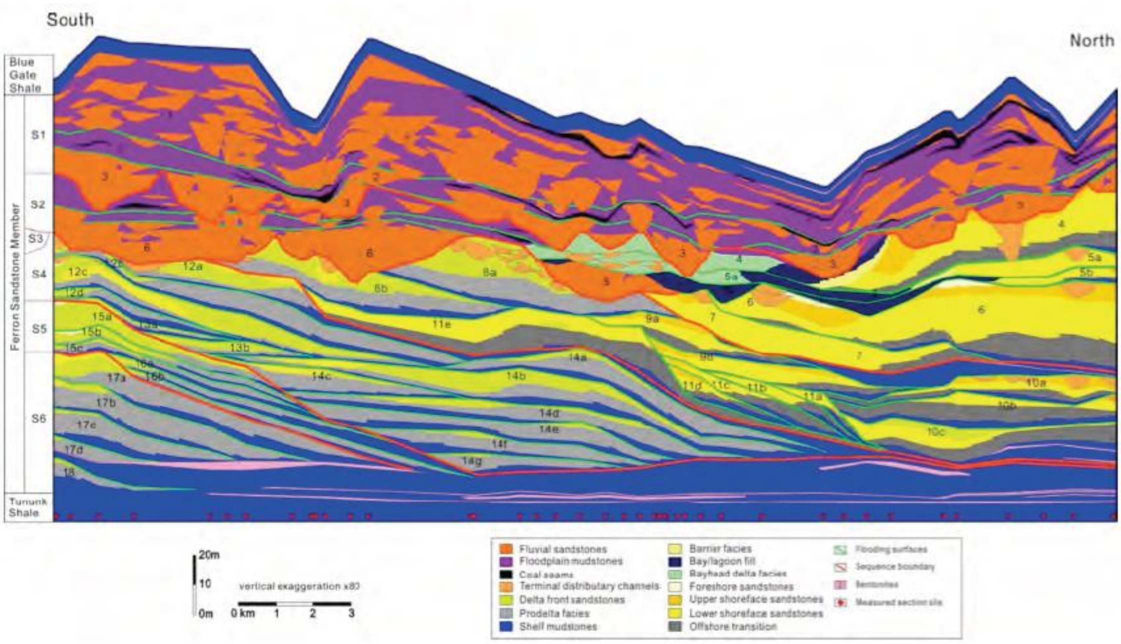

Figure. 9 Approximately depositional dip oriented regional stratigraphic cross section through the Ferron Notom delta. The Ferron Notom delta wedge contains 6 sequences, 18 parasequence sets, 43 parasequences. Cross section by Yijie Zhu with contributions by Weiguo Li.

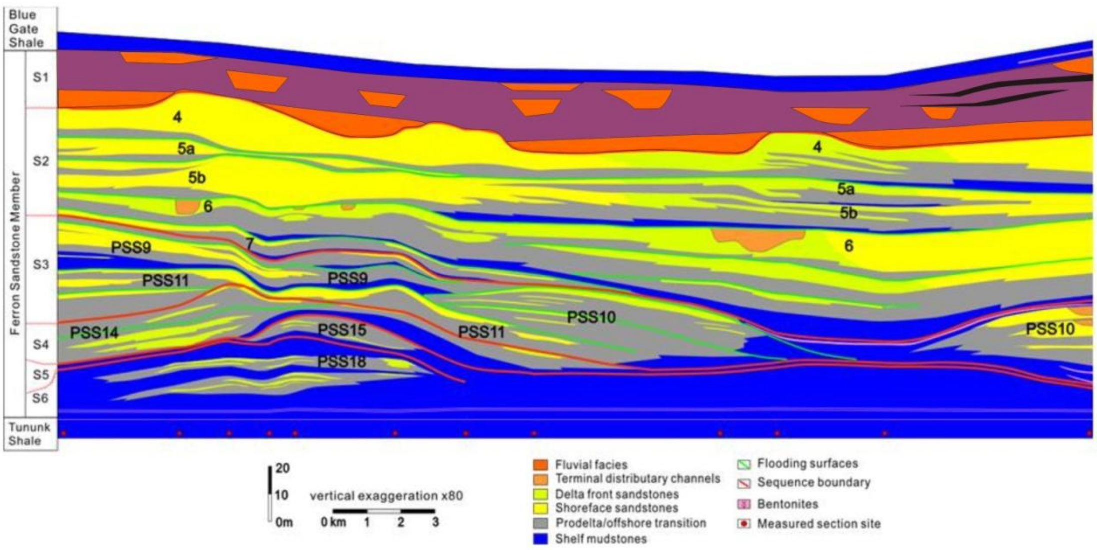

Figure. 10 Strike view of regional stratigraphic cross section. Revised version of figure based on Li, (2011).

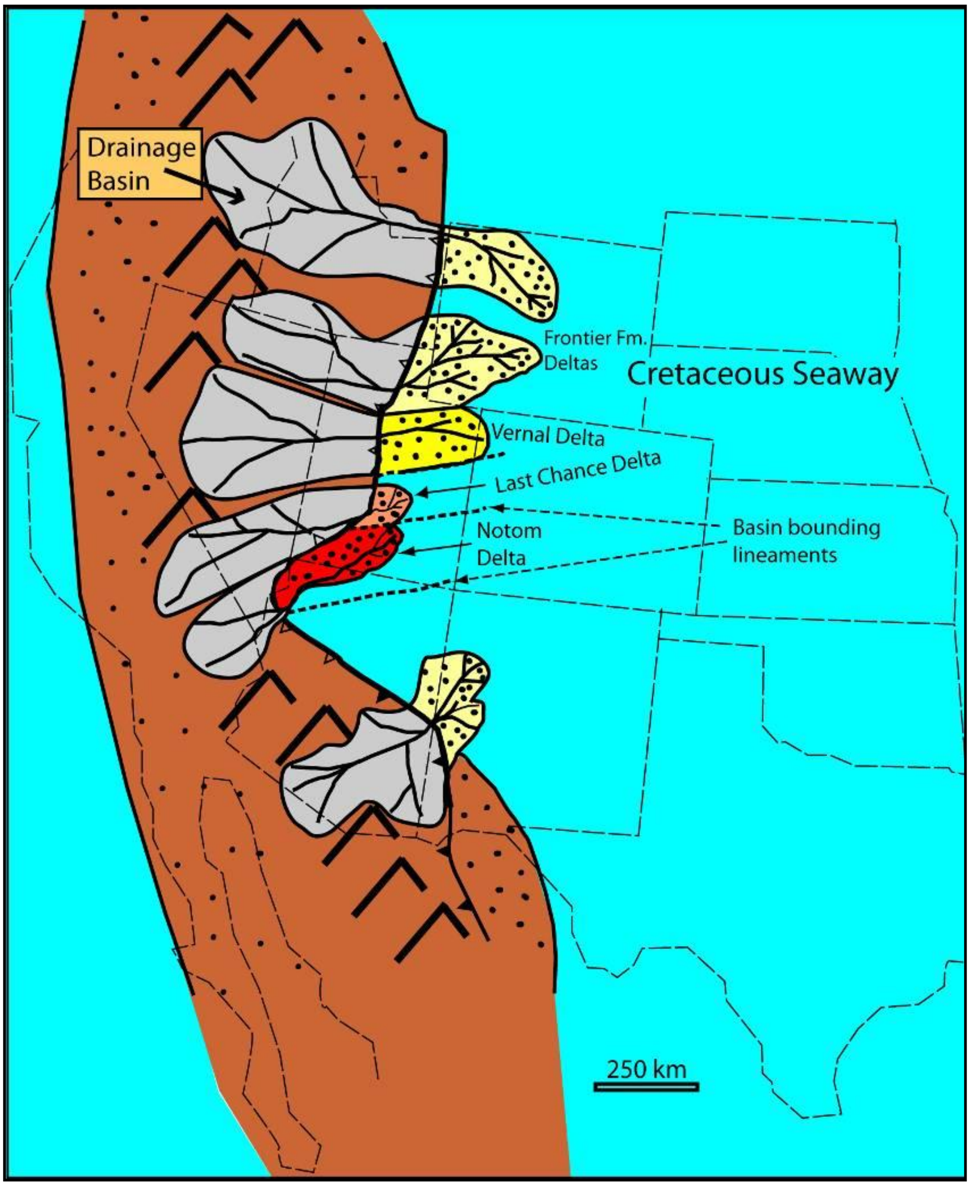

Figure. 11 Paleogeographic reconstruction of mid-Cretaceous clastic wedges. Figure from Bhattacharya and Tye (2004).

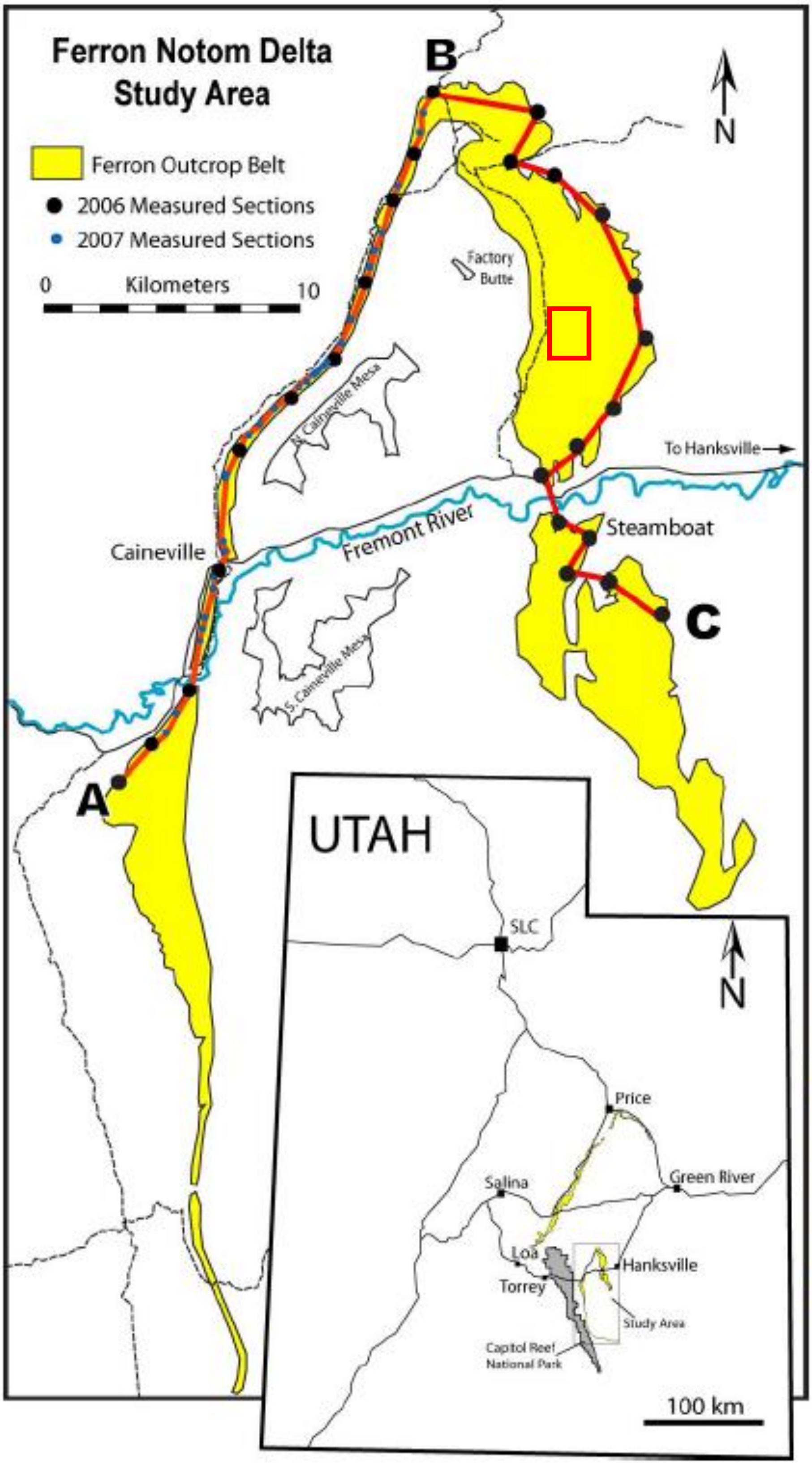

Figure. 12 Base map of the study area.

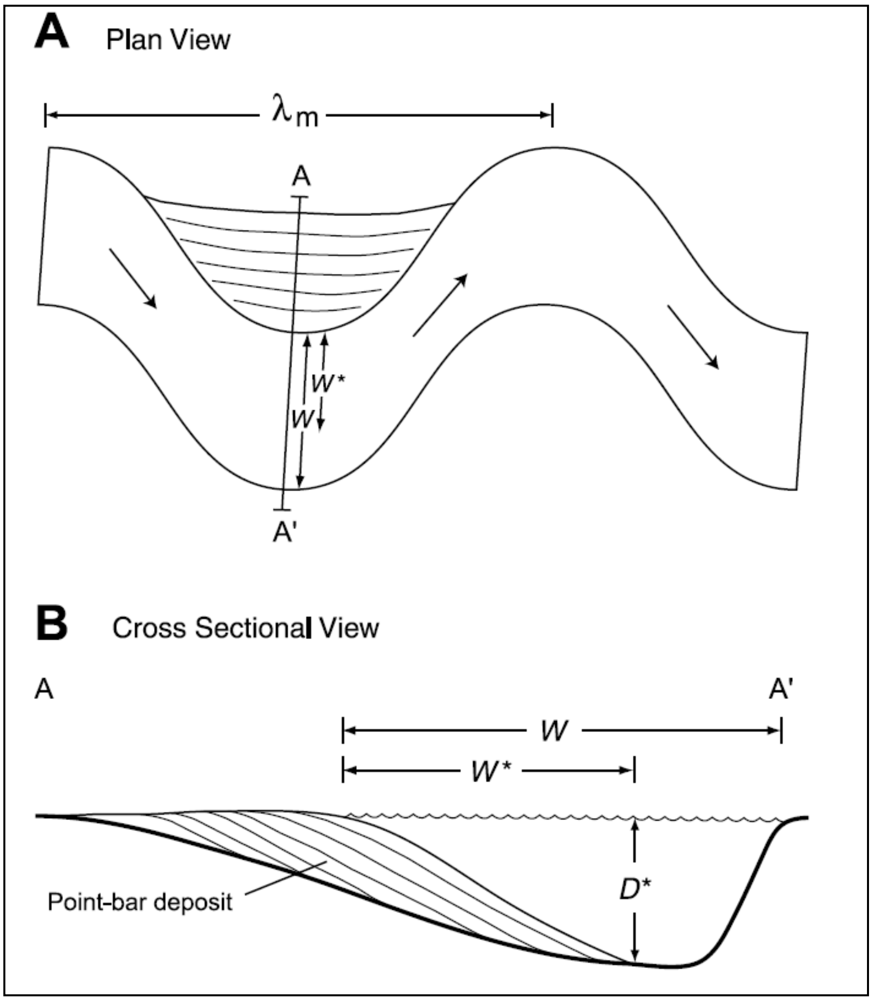

Figure. 13 Schematic illustration of a meander bend in (A) plan view and (B) cross sectional view. Geomorphic parameters include bankfull channel width (W) and meander wavelength (λm). Bankfull channel depth and width are estimated from point-bar deposits in outcrop using the point-bar thickness (D*) and horizontal length of lateral-accretion surfaces (W*). Based on Lorenz et al. (1985).

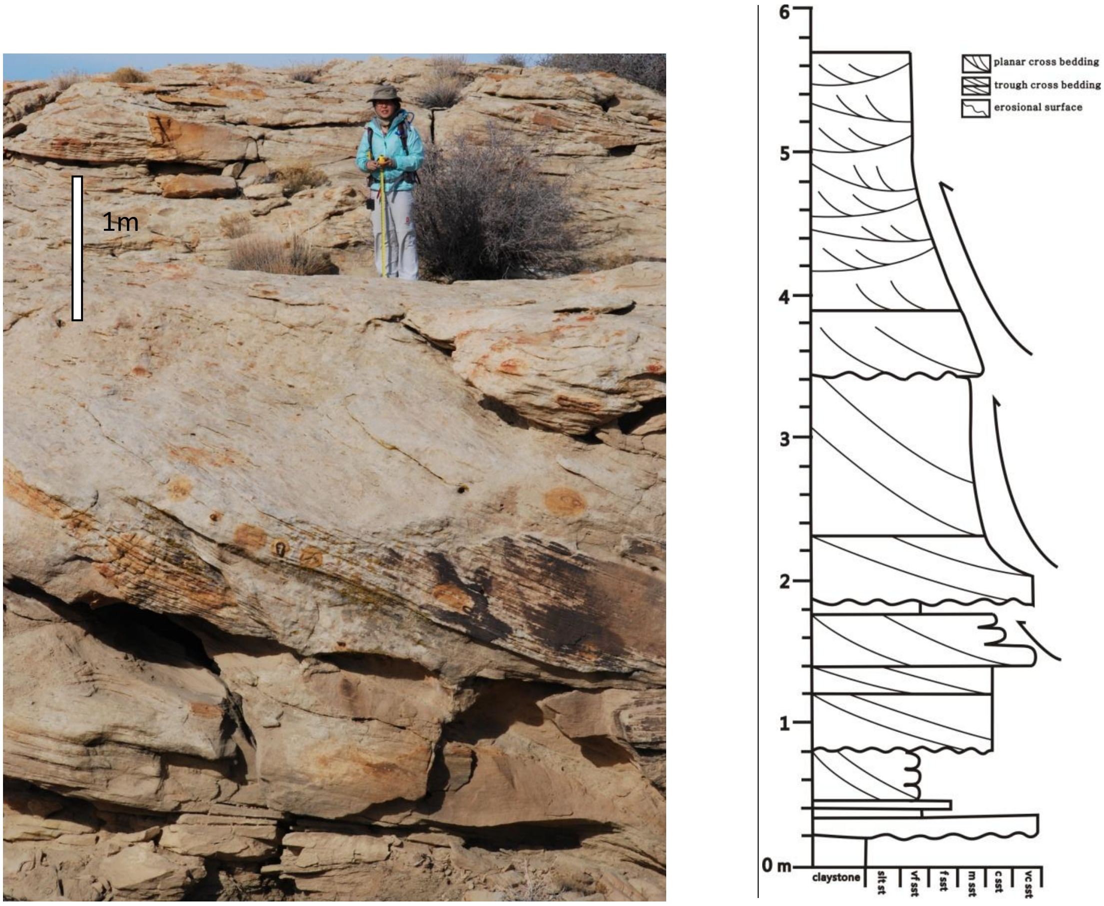

Figure. 14 Thick sandstone bodies with unit bar in the middle and compound bar on top.

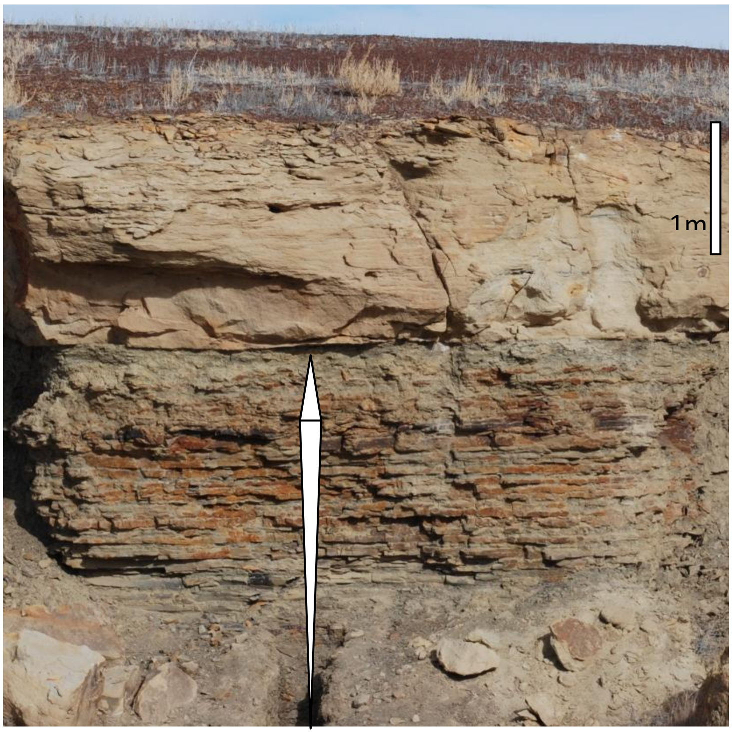

Figure. 15 Channel margin deposits with flood plain deposits preserved below

Figure. 16 Close-up photos of lacustrine facies underlying channel fill deposits.

Figure. 17 Rib and furrow structure on top of meander scroll.

Figure. 18 *Beaconites* burrows on top of channel margin deposits.

References

Adams, M. M., and Bhattacharya, J.P., 2005, No change in fluvial style across a sequence boundary, Cretaceous Blackhawk and Castlegate Formations of central Utah, U.S.A.: Journal of Sedimentary Research, v. 75, p. 1038-1051.

Barton, M. D., Angle, E. S., and Tyler, N., 2004, Stratigraphic architecture of fluvial-deltaic sandstones from the Ferron Sandstone outcrop, East-central Utah: , in T. C. Chidsey, R. D. Adams, and T. H. Morris, eds., The Fluvial-deltaic Ferron Sandstone: Regional to Wellbore Scale Outcrop Analog Studies and Applications to Reservoir Modelling: American Association of Petroleum Geologists Studies in Geology 50, p. 193-210

Bhattacharya, J. P, and Tye, 2004, Searching for modern Ferron analogs and application to subsurface interpretation, in Chidsey, T.C., Adams, R.D., and Merris, T.H., eds., Regional to Wellbore Analog for Fluvial Deltaic Reservoir Medeling, The Ferron of Utah: American Association of Petroleum Geologists, Studies in Geology 50, p. 39-57.

Bhattacharya, J. P, and MacEachern, J. A., 2009, Hyperpycnal rivers and prodeltaic shelves in the Cretaceous seaway of North America: Journal of Sedimentary Research, v. 79, p. 184-209.

Bridge, J. S., 1982, A revised mathematical model and FORTRAN IV program to predict flow in open-channel bends: Computers & Geosciences, v. 8, p. 91–95.

Bridge, J. S., Alexander, J., Collier, R. E. LL., Gawthorpe, R. L., and Jarvis, J., 1995, Ground-penetrating radar and coring used to study the large-scale structure of point-bar deposits in three dimensions: Sedimentology, v. 42, p. 839-852.

Bridge, J. S., and Tye, R. S., 2000, Interpreting the dimensions of ancient fluvial channel bars, channels, and channel belts from wireline-logs and cores: American Association of Petroleum Geologists, Bulletin, v. 84, p. 1205–1228.

Bridge, J. S., Jalfin, G.A., and Georgieff, S.M., 2000, Geometry, lithofacies, and spatial distribution of Cretaceous fluvial sandstone bodies, San Jorge Basin, Argentina: outcrop analog for the hydrocarbon-bearing Chubut Group. Journal of Sedimentary Research, v. 70, p. 314-359.

Bridge, J. S., 2003, Rivers and Floodplains: Oxford, U.K., Blackwell Science, 491 p.

Bridge, J. S., 2006, Fluvial facies models: recent developments, in Posamentier, H. W., and Walker, R. G., eds., Facies Models Revisited, SEPM, Special Publication 84, p. 83-168.

Corbeanu, R. M., Wizevich, M.C., Bhattacharya, J.P., Zeng, X., and McMechan, G.A., 2004, Three-dimensional architecture of ancient lower delta-plain point bars using ground penetrating-radar, Cretaceous Ferron Sandstone, Utah, in Chidsey, T.C., Adams, R.D., and Merris, T.H., eds., Regional to Wellbore Analog for Fluvial Deltaic Reservoir Medeling, The Ferron of Utah: American Association of Petroleum Geologists, Studies in Geology 50, p. 427-449.

Davidson, S. K., and Hartley, A. J., 2010, Towards a quantitative method for estimating paleohydrology from clast size and comparison with modern rivers: Journal of Sedimentary Research, v. 80, p, 688-702.

Forster, C. B., Snelgrove, S. H., and Koebbe, J. V., 2004 Modeling permeability structure and simulating fluid flow in a reservoir analog: Ferron Sandstone, lvie Creek area, east-central Utah, in T. C. Chidsey, R. D. Adams, and T. H. Morris, eds., The Fluvial-deltaic Ferron Sandstone: Regional to Wellbore Scale Outcrop Analog Studies and Applications to Reservoir Modelling: American Association of Petroleum Geologists Studies in Geology 50, p. 359-382

Gardner, M. H., 1995, Tectonic and eustatic controls on the stratal architecture of mid-Cretaceous stratigraphic sequences, central western interior foreland basin of North America, in S. L. Dorobek and G. M. Ross, eds., Stratigraphic evolution of foreland basins: Society for Sedimentary Geology (SEPM) Special Publication No. 52, p. 243-281.

Garrison, Jr., J.R., and Van den Bergh, T.C.V. ,2004, The High-resolution Depositional Sequence Stratigraphy of the Upper Ferron Sandstone Last Chance Delta: An Application of Coal Zone Stratigraphy, in T. C. Chidsey, R. D. Adams, and T. H. Morris, eds., The Fluvial-deltaic Ferron Sandstone: Regional to Wellbore Scale Outcrop Analog Studies and Applications to Reservoir Modelling: American Association of Petroleum Geologists Studies in Geology 50, p. 125-192.

Galloway, W. E., and Hobday, D.K., 1996, Terrigenous clastic depositional systems: Springer-Verlag, Heidelberg, 489 pp, p 151- 154

Jones, H.L., and Hajek, E.A., 2007, Characterizing avulsion stratigraphy in ancient alluvial deposits: Sedimentary Geology, v. 202, p. 124-137.

Knox, P. R., 1997, Application of Cretaceous Interior Seaway outcrop investigations to fluvial-deltaic reservoirs II — example from Gulf of Mexico reservoirs, Frio Formation, South Texas, in K. W. Shanley and R. F. Perkins, eds., Shallow marine and nonmarine reservoirs, sequence stratigraphy, reservoir architecture and production characteristics: Society for Sedimentary Geology (SEPM) Gulf Coast Section Foundation 18th Annual Research Conference, p. 127– 138.

Labreque, P. A., Jensen, J. L., Hubbard, S. M., 2011, Cyclicity in Lower Cretaceous point bar deposits with implications for reservoir characterization, Athabasca Oil Sands, Alberta, Canada: Sedimentary Geology, v. 242, p. 18-33.

Li, W., Bhattacharya, J. P., and Campbell, C., 2010, Temporal evolution of fluvial style in a compound incised-valley fill, Ferron “Notom Delta,” Henry Mountains Region, Utah (U.S.A.): Journal of Sedimentary Research, v. 80, p. 529-549.

Li, W., Bhattacharya, J. P., and Zhu, Y., 2011, Architecture of forced regressive systems tract in the Turonian Ferron “Notom Delta”, southern Utah, U.S.A.: Marian and Petroleum Geology, v. 28, p. 1517-1529.

Mackey, S. D., and Bridge, J.S., 1995, Three-dimensional model of alluvial stratigraphy; Theory and applications: Journal of Sedimentary Research, v. 65, p. 7–31.

Mackey, D. A., and Dalrymple, R. W., 2011, Dynamic mud deposition in a tidal environment: the record of fluid-mud deposition in the Cretaceous Blusky Formation, Alberta, Canada: Journal of Sedimentary Research, v. 81, p, 901-920.

Miall., A. D., 1994, Reconstructing fluvial macroform architecture from two-dimensional outcrops: examples from the Castlegate sandstone, Book cliffs, Utah: Journal of Sedimentary Research, v. B64, p. 146-158.

Miall, A. D., 2006, How do we identify big rivers, and how big is big: Sedimentary Geology 186, p. 39-50.

Mukherjee, D., Khan, S. D., and Sullivan, C., 2012, Upper Albian rudist buildups of the Edwards Formation in central Texas: A GPR-assisted reservoir analog study: Sedimentary Geology, 247-248, p. 71-81.

Pranter, M. J., Ellison, A.l., Cole, R.D., and Patterson, P. E., 2007, Analysis and modeling of intermediate-scale reservoir heterogeneity based on a fluvial point-bar outcrop analog, Williams Fork Formation, Piceance Basin, Colorado: American Association of Petroleum Geologists, Bulletin, v. 91, p 1025-1051.

Reijenstein, H. M., Posamentier, H. W., and Bhattacharya, J. P., 2011, Seismic geomorphology of inner-shelf fluvial, eustuarine, deltaic and marine sequences, Gulf of Thailand: American Association of Petroleum Geologists, Bulletin, v. 95, p. 1959-1990

Shanley, K. W., McCabe, P.J., and Hettinger, R., 1992, Tidal influence in Cretaceous fluvial strata form Utah, USA: a key to sequence stratigraphic interpretation: Sedimentology, v. 39, p. 905-930.

Shukla, U. K., Singh, I. B., Srivastava, P., and Sigh, D. S., 1999, Paleocurrent patterns in braid-bar and point-bar deposits: examples from the Ganga River, India: Journal of Sedimentary Research, v. 69, p. 992-1002.

Smith, D. G., Hubbard, S.M., Leckie, D.A., and Fustic, M., 2009, Counter point bar deposits: lithofacies and reservoir significance in the meandering modern Peace

River and ancient McMurray Formation, Alberta, Canada, Sedimentology, v. 56, p. 1655-1699.

Tye, R. S., 2004, Geomorphology: An approach to determining subsurface reservoir dimensions: American Association of Petroleum Geologists, Bulletin, v. 88, p. 1123-1147.

Van den Bergh, T. C. V., and Garrison, Jr., J. R., 2004, The geometry, architecture, and sedimentology of fluvial and deltaic sandstones wihin the upper Ferron Sandstone Last Chance Delta: implication for reservoir modeling, in T. C. Chidsey, R. D. Adams, and T. H. Morris, eds., The Fluvial-deltaic Ferron Sandstone: Regional to Wellbore Scale Outcrop Analog Studies and Applications to Reservoir Modelling: American Association of Petroleum Geologists Studies in Geology 50, p. 451-498.

Willis, B. J., 1989, Paleochannel reconstructions from point bar deposits: a three-dimensional perspective, Sedimentology, v. 36, p. 757-766.

Willis, B. J., 1993a, Bedding geometry of ancient point bar deposits, in Marzo, M., and Puigdefabregas, C., eds., Alluvial Sedimentation: International Association of Sedimentologists, Special Publication 17, p. 101–114.

Willis, B, J., and Tang, H., 2010, Three-dimentional connectivity of point bar deposits: Journal of Sedimentary Research, v. 80, p. 440-454.

Zhu, Y., 2010, Sequence stratigraphy and facies architecture of the Cretaceous Ferron Notom Delta complex, Southern Utah, USA: PhD Dissertation, University of Houston.

Zhu, Y., Bhattacharya, J. P., Li, W., Lapen, T.J., Jicha, B., and Singer, B., in press, High-frequency sequence stratigraphy of the Turonian Ferron Notom Deltaic Complex, South-Central Utah: Evidence for glacio-eustasy? Journal of Sedimentary Research.